Volume 68, Issue 3, 2024
Journal of Scientific Research
of
The Banaras Hindu University

Structural Simulation and Investigation of Propagation Characteristics of Photonic Crystal Fibers for Efficient Transmission and Delivery of Ultrashort Optical Pulses

Priyanka Talukdar[1], Devika Phukan[2], Subrata Hazarika[3]

1. Department of Physics, Royal Global University, Guwahati 781035, Assam,
mail id: priyankatalukdar17031995@gmail.com
2. Department of Physics, Royal Global University, Guwahati 781035, Assam,
mail id: devikaphukan@gmail.com
3. Department of Physics, Diphu Campus, 782462, Assam,
mail id: hazarikasubrata@rediffmail.com

Abstract:

Over the years, various studies have been done on the structural designing and analysis of photonic crystal fibers. Their unique specialty is their flexibility in designing and excellent optical properties. This study simulates PCFs to come up with the parameters favoring for an efficient transmission. Finite Difference Time Domain (FDTD) method is used for simulations and to characterize the optical parameters of the designed fiber. The effect of the structural parameters of the fiber on the transmission, confinement loss and dispersion is studied. Tailoring of zero dispersion wavelengths by changing the diameter of air holes, pitch and number of air hole rings has been investigated.

Keywords: Confinement loss, Finite Difference Time Domain, Hollow Core Photonic Crystal Fibers, optical properties, optical parameters,

I. INTRODUCTION

The cladding region of Photonic bandgap fiber is composed of a periodic array of microscopic air holes. Light transmits via the photonic bandgap mechanism through these fibers [1]. There are two types of Photonic bandgap fibers: Bragg fiber [2], [3]and hollow core photonic crystal fiber (HC-PCF) [4], [5], [6]. Photonic crystal fibers (PCFs) have proven themselves to be better than conventional fibers over time, with their distinctive features and numerous implementations in different fields starting from telecommunication, medical to sensing applications. The PCF's core may be hollow or solid. Light is guided utilizing the modified total internal reflection (TIR) phenomenon in a solid-core PCF. The core and equivalent index of the cladding have a positive refractive index difference in a solid core PCF. In contrast, hollow core PCF uses a photonic band gap (PBG) mechanism for light steering and has a negative refractive index difference between the core and cladding. These structures demonstrate the new characteristics of low loss and perpetual single mode propagation. These fibers stand outs conventional optical fibers because of their unique feature of flexibility in designing. The possible variations in their structural parameters allow us to find out the appropriate configuration of the fiber for low loss transmission. The crystal like structure

DOI: 10.37398/JSR.2024.680306

of these fibers provides them with few uncommon properties, like single-mode operation, large mode areas, high nonlinear performance, tunable dispersion, large bandwidth, flexibility, high tensile strength and low absorption [7], [8]. PCFs also show extraordinary performance in light guidance in air,dispersion and enhancement of non linear effect [9]. The properties of a PCF can be altered by altering the fiber design, like changing the air hole size or pattern. Raman scattering and self-phase modulation cause short, high-power pulses in conventional optical fibers to be broken apart. According to studies, PCFs can be utilized to deliver high power, ultra-short light pulses over considerably greater distances without experiencing severe temporal distortion [10]. Researchers have used PCF for a variety of purposes, including supercontinum generation [11], Raman scattering [12], fiber laser [13], optical sensors [14], and spectroscopy [15] due to its superior qualities over conventional optical fibers. This study simulates PCFs with varying parameters to come up with the one with the most efficient transmission characteristics. Simulation and modeling of various fibers allows us to explore their optical parameter profiles without the time consuming methods of fiber fabrications. Controlling dispersion in PCFs is a critical issue for practical applications in optical communication systems, dispersion compensation and non linear optics. In general, numerical techniques like the finite difference approach [16], finite element method (FEM) [17], block-iterative frequency-domain method [18], and plane wave expansion method [19], [20] are used to accurately simulate and optimize photonic crystal structures. Finite Difference Time Domain (FDTD) method is used in this study for simulations and to characterize the optical parameters of the designed fiber. FDTD method with anisotropic perfectly matched layers is used to examine the dispersion characteristics and confinement losses in a PCF. The FDTD method can be applied predominantly for solving complex electromagnetic computations. The FDTD algorithm has turned out to be a major appliance in nanophotonics over the past decade because of its ability to deal with complex structures [21]. The integrated design of this simulator provides scripting capability, advanced post processing through various time and frequency profile monitors, optimizations, sweeps, far field analysis, modal analysis, and many more such options, enabling designers to accurately design various models. This method simulates the set of Maxwell's equations evolving with time by using the finite difference approximation and divides space and time into a regular grid [22].

II. METHODOLOGY

Partial differential equations in the time and space domains can be solved numerically using the software Finite Difference Time Domain (FDTD) simulation. It has shown to be a potent tool for modeling the propagation of electromagnetic waves and has applications in optics, electromagnetic, photonics, and acoustic engineering, and many others. Studies of complicated phenomena involving wave interactions with structures and materials benefit greatly from the use of FDTD models. The methodology divides the time and space domains into tiny grid cells, enabling a time-stepping procedure that simulates the evolution of waves. FDTD simulations can precisely simulate the effects of wave propagation, reflection, diffraction, dispersion and scattering by updating the electric and magnetic fields within each grid cell.

We have modeled pulse propagation inside the fiber using the nonlinear envelope equation, from which the propagationequation can be written as [23]

$$\frac{\partial \mu}{\partial \in} = \sum_{n=2}^{4} - (i)^{n-1} \frac{L_{ds}}{n! L_{ds}^{(n)}} \frac{\partial^n \mu}{\partial \tau^n} + i \left(1 + \frac{i}{\omega_o \tau_p} \frac{\partial}{\partial \tau}\right) p^{nl} \quad \textbf{(1)}$$

Where $\tau = \frac{t - \frac{z}{v_g}}{\tau_p}$ is the retarded frame time normalized to the input pulse width τ_p, L_{ds} is the dispersion length and ω_o is the central frequency. The n^{th} order dispersion length is given as

$$L_{ds}^{(n)} = \frac{\tau_p^n}{\beta_n} \quad \textbf{(2)}$$

A mode of PCF is characterized by its propagation constant β, or by its effective index n neff both related as

$$n_{eff} = \frac{\beta}{k_0} \quad (3)$$

The dispersion parameter is computed from the real part of the effective index, given as [24],

$$D = \frac{-\lambda}{c} \frac{\partial}{\partial \lambda^2} Re\,(n_{eff}) \quad (4)$$

where c is the velocity of light in vacuum and *Re* stands for the real part of η_{eff} which is the effective index.

The dispersion of the guided modes is caused by both material and waveguide dispersion, just like in regular waveguides. The noteworthy characteristics of PCFs are that the waveguide dispersion may be greatly altered by varying the geometrical parameters, specifically the locations and sizes of the air holes. Another important consideration while designing a PCF with a limited number of air holes is the confinement loss. Due to the limited number of air holes, the guided light penetrates to the cladding region, leading to confinement loss. The confinement loss is derived from the effective index value, given as

$$L = 8.686\ \mathrm{Im}\,[k_0 n_{eff}] \quad (5)$$

Where *Im* stands for the imaginary part.

III. PROPOSED FIBER STRUCTURE

The simulations are based on the FDTD method [25] and the boundary condition considered for the study is perfectly matched layer (PML) [26], [27],[28].The method approximates the cross sectional area of the fiber proposed using a rectangular uniform mesh grid with a mesh step of 0.25 nm. Stretched coordinate perfectly matched layer condition is set up as the boundaries of the fiber. Conformal mesh refinement is applied to approach precise measurements and to diminish errors in the simulation. Thewavelength considered for the study is in the range 1.3-2 μm. The designed fiber supports the fundamental mode and also some higher order modes. But, only the fundamental mode is considered for exploring the propagation features of the fiber. The hole to hole distance, called the hole pitch, is denoted by 'Λ'. The diameter of the air hole in each ring of the cladding is denoted by 'd', for all types of fiber designed. The background material for all types of fiber designed is pure silica and the refractive index is determined using the Sellmeier equation [29].

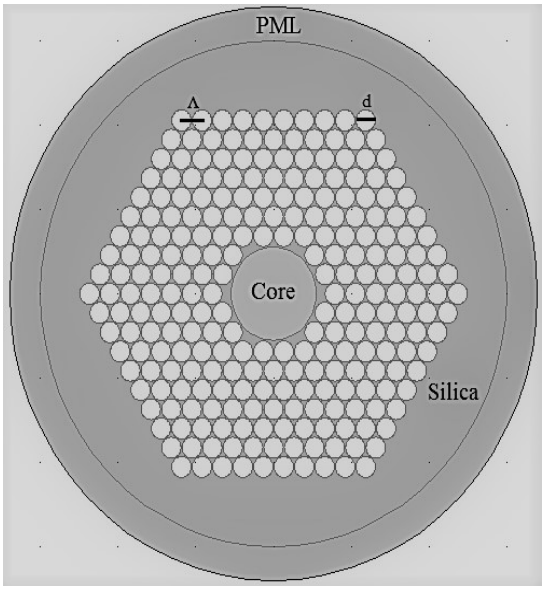

Fig 1: *Pictorial representation of the designed PCF with background material silica and perfectly matched layer (PML) as boundary condition*

IV. SIMULATIONS AND RESULTS

The FDTD method applies the finite difference approximation to convert Maxwell's equations into a numerical eigen value problem. The mode propagation constant, β can be obtained from the updated equations. The eigen value equations can be solved to determine β, for a considered geometry of the PCF. The effective index (neff) of the mode can be calculated by the equation (3). FDTD provides various simulation objects to define simulation parameters like mesh size and boundary conditions. FDTD also introduces the conformal mesh technology that can be used to improve simulation accuracy. There are different time and frequency domain monitors to visualize results of the simulation. We have considered a photonic crystal fiber with varying array lattice structure. A Gaussian pulse with a wavelength centered at 1.65 μm is considered as the input source. The confinement loss as a function of wavelength is shown for the different lattice structure considered.

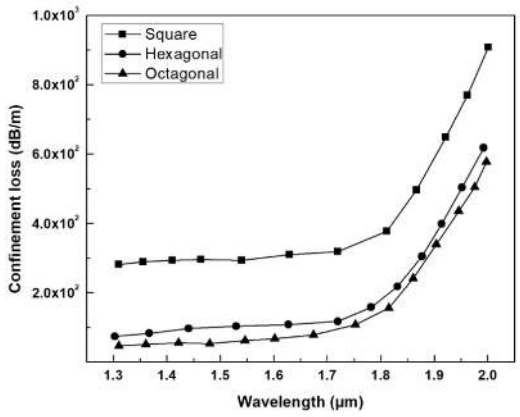

Fig 2: Confinement loss (db/km) as a function of wavelength (μm) for the different structure of PCFs: Square, Hexagonal and Octagonal

For the structural parameters fixed at Λ= 2.6 μm and d = 0.5 μm, we have depicted the variation in the confinement loss with respect to wavelength for a square, an octagonal and a hexagonal lattice shaped fiber. Since octagonal-PCF showed the lowest confinement loss (less than 1 dB/km for the wavelength range less than 1.6 μm), so the further investigation is done considering the designed Octagonal-PCF.

The transmission graph as a function of wavelength was studied by changing the air hole ring numbers of the designed octagonal lattice fiber as seen in figure 3. It was found that with the increase in the number of air hole rings, the transmission increases rapidly. The peak point of transmission lies around 1.62 μm, which is the centered wavelength of the input pulse that does not varies with the change in ring numbers.

Figure 4 shows that as the number of rings increases, there is a decrease in the difference between the consecutive dispersion curves, for various wavelength values considered. The consecutive dispersion curves can be seen converging to a fixed value

with an increase in the ring number. The rate of convergence is found to be more in lower wavelength range as compared to higher wavelength range. The dispersion characteristics become more uniform and predictable as the number of rings increases. Figure 5 shows that altering the air hole diameter has an impact on the dispersion profile and that increasing the value of'd' allows the index guiding PCFs to better regulate their dispersion characteristics. Since, dispersion is strongly wavelength dependent in nature; it can be seen shifting from positive (indicating normal dispersion) to negative (indicating anomalous dispersion) value as it goes from shorter to longer wavelength region.

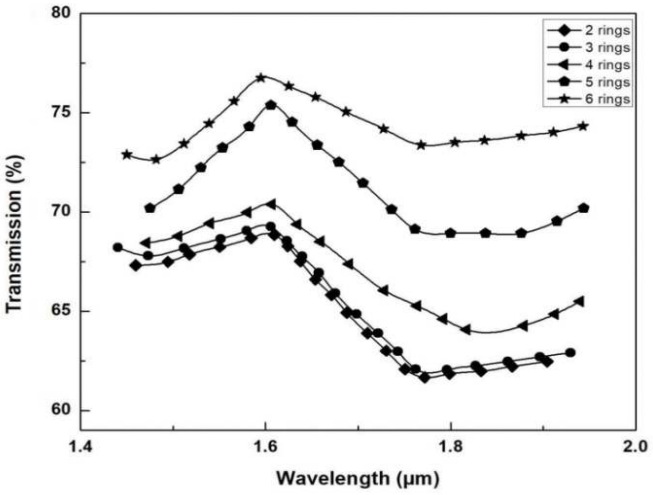

Fig 3: Transmission vs. Wavelength plot for different number of air hole rings of the fiber

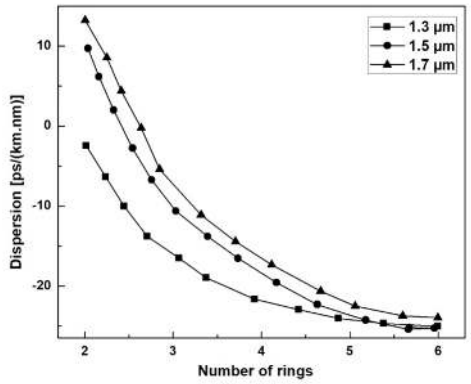

Fig 4: Dispersion [ps/ (km.nm)] as a function of number of rings for three different wavelengths is considered

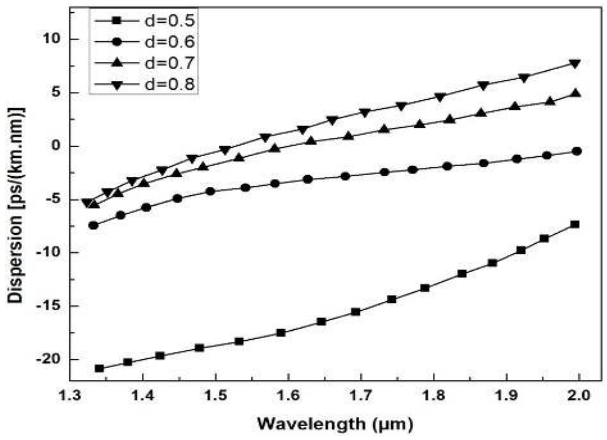

Fig 5: Dispersion curve as a function of wavelength for varying values of air hole radius (d), keeping the number of rings fixed at 6

Figure 6 shows that designing a flattened dispersion curve in PCFs for a wide wavelength range is conceivable by adding additional air hole rings in the PCF. The 4 ring PCF showed a flattened dispersion of 0 ±0.5 ps/(km.nm) for the wavelength range 1.39-1.91 μm. The designed 5 and 6 ring PCF showed a flattened dispersion of 0± 0.4 ps/(km.nm) and 0± 0.3 respectively, for the wavelength range of 1.34-1.87 μm and 1.42-1.85 μm respectively. The addition of extra air hole rings in the PCF enables the design of a flattened dispersion curve, i.e., the dispersion of the PCF remains constant over a wide range of wavelength. Dispersion value closer to zero indicates minimal pulse distortion and pulse spreading for light signals within the specified wavelength ranges. Designing of PCFs with flattened dispersion curves enables improved control and manipulation of light signals for a range of applications that requires stable and high quality optical transmission. These PCFs exhibiting nearly ultra flattened zero dispersion and can be utilized for super continuum generation, soliton pulse transmission and high power pulse delivery.

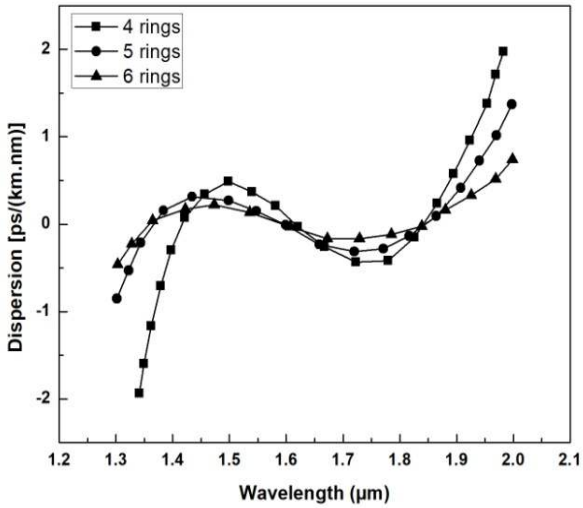

Fig 6: Dispersion curve as a function of wavelength for the designed fiber with 4, 5 and 6 air hole ring

V. CONCLUSION

Finite Difference Time Domain method with anisotropic perfectly matched layers is used to examine the dispersion characteristics and confinement losses in a PCF. The impacts of structural parameters on the pulse transmission were also investigated. Confinement loss and dispersion curves are examined and compared with varying number of rings and air hole size in the cladding. Studying the Group Velocity Dispersion (GVD) characteristics of the proposed fiber shows that it shifts from negative at shorter wavelengths to positive values at longer wavelengths. This behavior is advantageous in applications like soliton pulse transmission, where a balance between dispersion and non linearity is required to maintain pulse shape and prevent distortion. We have designed a PCF with 6 air hole rings achieving a flattened dispersion of 0 ± 0.3 ps/(km.nm) in the wavelength range of 1.42-1.85 μm. The designed fiber exhibits minimal variation in group velocity with respect to wavelength within this range. This characteristic is desirable in applications like dispersion compensation, where the goal is to counteract the pulse spreading effect caused by GVD. The study contributes to various engineering applications in the field of optical communication and photonics. These applications include transmission of ultra-short and high energy optical pulses, wideband supercontinum, dispersion compensation, soliton pulse transmission and wavelength division multiplexing transmission employing PCFs. The findings of this study provide valuable insights for designing PCFs with specific dispersion properties to meet the requirements of these applications.

REFERENCES

1. Knight J. K, Broeng J., Rusell P. (1998), Science 282, 1476-1478
2. Dupuis A., Stoeffler K, Ung B, Dubois C, Skorobogatiy M (2011) Journal of the Optical Society of America B 28, 896-907
3. Hong B, Swithenbank M, Somjit N, Cunningham J, Robertson I (2017) IEEE Transactions on Terahertz Science and Technology 8, 90-99
4. Geng Y. F., Tan X Wang P, Yao J. Q (2008) Applied Physics B 91, 333-336
5. Broeng J, Sondergaard T, Barkou S. E, Barbeito P. M, Bjarklev A (1999), Journal of Optics A: Pure and Applied Optics 1,477–482
6. Chugh S, Gulistan A, Ghosh S, Rahman B.M.A (2019), Optics Express 27, 36414-36425
7. Sanjaykumar G, Sudipta M, Varshneya S.K, Sahub P.K (2013) Optik 124, 3730-3733
8. Sharma P, Vyas K (2015), international Journal of modern communication technologies research 3, 1-3
9. Ahmed K, Morshed M (2016), Sensing and bio sensing research 7, 1-6
10. Blanch A, Knight J.C, Wadsworth W.J (2000), Optics letters 25, 1325
11. Wardsworth W.J, Blanch A, Knight J.C, Birks T.A, Rusell J (2002), Opt. Soc. Am. B, 19(9), 2148-2155
12. Benabid, Knight J.C, Antonopoulos G., Rusell J (2002), science 2989(5592), 399-402
13. Cheo P. K, Liu A, King G. G. (2001), IEEE Photonics Tech. Lett., 13(5), 439-441
14. De M., Gangopadhay T.K, Singh V.K (2019), Sensors 19(3), 464
15. Holzwarth R, Udem T, Knight J.C, Wadsworth W. J, Rusell J. (2000), Phys. Rev. Lett 85(11), 2264-2267
16. Yu C.P, Chang H.C (2004), Opt. Quantum Electronics, 36(1-3), 145-163
17. Cucinotta A, seller S, vincetti L., Zoboli M (2002), IEEE Photonics Tech. Letters 14(11), 1530-1532
18. Johnson S.G, Joannopoulos J.D. (2001), opt. Express 8(3), 173-190
19. Shi S, Chen C, Prather D. W (2004), Opt. Soc. America A 21, 1769-1775
20. Norton R.A, Scheichl R (2013), Appl. Numer. Math. 63, 88-104
21. Kuiri B, Dutta B, Sarkar N, Patra A.S (2022), Optical fiber technology 68
22. Mussina R., selviah D.R, Fernandez F.A (2014), Progress in electromagnetic research, 145, 93-113
23. Buczynski R ()2004), Photonic crystal fibers, Acta Physica Polonica A 106, 141-168
24. Saitoh K, Koshiba M, Hasegawa T (2003), Optics Express 11, 843-852
25. Sullivan D.M, (2013) Electromagnetic simulation using the FDTD method, John Wiley sons
26. Berenger J.P (1994), Journal of computational physics, 114, 185-200
27. Agrawal A, Sharma A (2004), Applied Optics 43, 4225-4231
28. Shin W., Fan S (2012), Journal of Computational Physics, 231, 3406-3431
29. Saitoh K, Koshiba M, Hasegawa T (2003), Optics express 11(8), 843-85

Table I : Wavelength (μm) vs. Confinement loss (dB/km) corresponding to figure 2

Sl no.	Wavelength (μm)	Confinement loss (dB/km)	Wavelength (μm)	Confinement loss (dB/km)	Wavelength (μm)	Confinement loss (dB/km)
1	1.31	281.47	1.31	281.47	1.31	281.47
2	1.36	288.34	1.36	288.34	1.36	288.34
3	1.41	292.91	1.41	292.91	1.41	292.91
4	1.46	295.20	1.46	295.20	1.46	295.20
5	1.54	292.91	1.54	292.91	1.54	292.91
6	1.63	308.93	1.63	308.93	1.63	308.93
7	1.72	318.08	1.72	318.08	1.72	318.08
8	1.81	377.58	1.81	377.58	1.81	377.58
9	1.87	496.57	1.87	496.57	1.87	496.57
10	1.92	647.60	1.92	647.60	1.92	647.60

Table II: Wavelength (μm) vs. transmission (%) corresponding to figure 3

Sl no.	Wavelength (μm)	Transmission (%) (2 rings)	Wavelength (μm)	Transmission (%) (3 rings)	Wavelength (μm)	Transmission (%) (4 rings)	Wavelength (μm)	Transmission (%) (5 rings)	Wavelength (μm)	Transmission (%) (6 rings)
1	1.36	69	1.36	69	1.36	70	1.36	72	1.36	75
2	1.39	68	1.39	69	1.39	69	1.39	71	1.39	74
3	1.46	67	1.44	68	1.47	68	1.48	70	1.45	73
4	1.49	67	1.47	68	1.51	69	1.51	71	1.48	73
5	1.62	68	1.62	69	1.66	69	1.63	75	1.62	76
6	1.64	68	1.64	68	1.69	67	1.66	73	1.65	76
7	1.65	67	1.66	67	1.73	66	1.68	73	1.69	75
8	1.67	66	1.68	66	1.76	65	1.71	71	1.73	74
9	1.71	64	1.72	64	1.82	64	1.76	69	1.80	73
10	1.75	62	1.76	62	1.91	65	1.84	69	1.88	74

Table III: Dispersion [ps/ (km.nm)] vs. number of rings corresponding to figure 4

Sl no.	Number of rings	Dispersion [ps/(km.nm)]	Number of rings	Dispersion [ps/(km.nm)]	Number of rings	Dispersion [ps/(km.nm)]
1	2.02	-2.47	2.04	9.71	2.01	13.24
2	2.24	-6.37	2.16	6.18	2.25	8.56
3	2.45	-10.05	2.33	2.00	2.41	4.38
4	2.71	-13.80	2.54	-2.76	2.64	-0.24
5	3.07	-16.54	2.76	-6.73	2.85	-5.43
6	3.37	-18.99	3.03	-10.62	3.32	-11.13
7	3.92	-21.65	3.39	-13.80	3.71	-14.44
8	4.42	-22.95	3.73	-16.54	4.12	-17.33
9	4.87	-24.03	4.17	-19.56	4.67	-20.65
10	5.38	-24.68	4.63	-22.30	5.06	-22.52

Table IV: Dispersion [ps/ (km.nm)] vs. wavelength (μm) corresponding to figure 5

Sl no.	Wavelength (μm)	Dispersion [ps/(km.nm)] (d= 0.5)	Wavelength (μm)	Dispersion [ps/(km.nm)] (d=0.6)	Wavelength (μm)	Dispersion [ps/(km.nm)] (d=0.7)	Wavelength (μm)	Dispersion [ps/(km.nm)] (d=0.8)
1	1.31	-21.52	1.30	-8.17	1.30	-6.55	1.30	-5.99
2	1.34	-20.85	1.33	-7.44	1.33	-5.54	1.32	-5.26
3	1.42	-19.67	1.41	-5.76	1.40	-3.52	1.39	-3.24
4	1.53	-18.33	1.49	-4.25	1.45	-2.62	1.47	-1.11
5	1.69	-15.58	1.63	-3.13	1.58	-0.26	1.62	1.59
6	1.74	-14.40	1.68	-2.84	1.63	0.41	1.66	2.48
7	1.79	-13.33	1.68	-2.84	1.68	0.86	1.71	3.21
8	1.84	-11.99	1.73	-2.45	1.73	1.53	1.76	3.83
9	1.88	-10.98	1.77	-2.23	1.73	1.53	1.81	4.67
10	1.95	-8.68	1.87	-1.61	1.82	2.43	1.92	6.47

Table V: Dispersion [ps/ (km.nm)] vs. wavelength (μm) corresponding to figure 6

Sl no.	Wavelength (μm)	Dispersion [ps/(km.nm)] (4 rings)	Wavelength (μm)	Dispersion [ps/(km.nm)] (5 rings)	Wavelength (μm)	Dispersion [ps/(km.nm)] (6 rings)
1	1.34	-1.94	1.30	-0.85	1.30	-0.46
2	1.35	-1.60	1.32	-0.53	1.33	-0.23
3	1.36	-1.17	1.34	-0.21	1.36	0.04
4	1.38	-0.70	1.38	0.16	1.42	0.17
5	1.40	-0.30	1.43	0.31	1.47	0.22
6	1.42	0.08	1.50	0.27	1.54	0.14
7	1.46	0.34	1.55	0.15	1.61	-0.03
8	1.50	0.49	1.60	-0.01	1.67	-0.17
9	1.58	0.21	1.72	-0.31	1.79	-0.12
10	1.62	-0.03	1.77	-0.28	1.84	-0.02